Inverse Seesaw Neutrino Signatures at the LHC and ILC

A. Das – University of Alabama
N. Okada – University of Alabama

Citation of published version:

Das, A., Okada, N. (2013): Inverse Seesaw Neutrino Signatures at the LHC and ILC. *Physical Review D,* 88(11).
DOI: https://doi.org/10.1103/PhysRevD.88.113001

PHYSICAL REVIEW D **87,** 065009 (2013)

Higgs-lepton inflation in the supersymmetric minimal seesaw model

Masato Arai,[1,*] Shinsuke Kawai,[2,3,†] and Nobuchika Okada[4,‡]

[1]*Fukushima National College of Technology, Iwaki, Fukushima 970-8034, Japan*
[2]*Institute for the Early Universe (IEU), 11-1 Daehyun-dong, Seodaemun-gu, Seoul 120-750, Korea*
[3]*Department of Physics, Sungkyunkwan University, Suwon 440-746, Korea*
[4]*Department of Physics and Astronomy, University of Alabama, Tuscaloosa, Alabama 35487, USA*

(Received 8 January 2013; published 12 March 2013)

We investigate a scenario of cosmological inflation realized along a flat direction of the minimal seesaw model embedded in supergravity with a noncanonical R-parity violating Kähler potential. It is shown that with appropriate seesaw parameters the model is consistent with the present observation of the cosmological microwave background as well as with the neutrino oscillation data. It is also shown that the baryon asymmetry of the Universe can be generated through leptogenesis. The model favors supersymmetry breaking with the gravitino as the lightest superparticle, and thus indicates the gravitino dark matter scenario. An interesting feature of this model is that the seesaw parameters are constrained by the cosmological microwave background spectra. The 2-σ constraints from the 9-year WMAP data yield a mild lower bound on the seesaw mass scale $\gtrsim$ TeV. We expect that the observation by the Planck satellite will soon provide more stringent constraints. The phenomenological and cosmological implications of the R-parity violation are also discussed.

DOI: 10.1103/PhysRevD.87.065009 PACS numbers: 12.60.Jv, 14.60.St, 98.80.Cq

I. INTRODUCTION

In cosmology, the particle physics origin of inflation remains as an unsolved problem. In search of a realistic inflationary model one may take two possible approaches. One is the top-down approach, starting with a unifying theory including gravity. String cosmology [1], loop quantum cosmology [2], and cosmological model building based on F-theory grand unification [3] fall into this category. The top-down approach is an ambitious program to build a consistent scenario from the first principles. The other is the bottom-up approach, that is, to investigate embedding of inflation into particle physics models that are confirmed at low energies, starting from the Standard Model (SM) and its various extensions. The bottom-up approach is advantageous in predictability and falsifiability. In view of the remarkable progress and ever-increasing precision in observational cosmology [4,5] one could hope that in the near future observation will be able to narrow SM-based inflationary models down to a handful of candidates. In this paper we take the bottom-up approach and propose a model of inflation, which we believe to be a promising and testable candidate.

Recently, there has been a revival of interest in cosmological inflation within the SM, where the Higgs field, nonminimally coupled to gravity, is identified as an inflaton [6–19] (see also Refs. [20–24] for older proposals of nonminimally coupled inflation models). Interestingly, it requires the Higgs mass to be 126–194 GeV, consistent with the mass scale suggested by the Large Hadron Collider experiments [25,26]. The Higgs inflation model also predicts small tensor-mode perturbation that fits remarkably well with the present-day cosmological microwave background (CMB) observation. The success of the model comes at the cost of an extremely large coupling $\xi \sim 10^4$ between the Higgs field and the background curvature, which could lead to the violation of the unitarity bound [14–19] (for the controversy see also Refs. [11–13,27,28]). Also, the model suffers from the usual hierarchy problem of the SM, namely the Higgs potential is destabilized due to radiative corrections [8,9,12,13]. As is well known, the hierarchy problem is solved, or at least tamed, by introducing supersymmetry. Supersymmetric versions of the Higgs inflation model were considered in Refs. [27–29], and it was shown that while embedding into the minimal supersymmetric Standard Model (MSSM) is not possible (as the field content is too restrictive), the next-to-minimal supersymmetric SM successfully accommodates Higgs inflation. Embedding into supersymmetric grand unified theory [30] (see also Ref. [31]) and other supersymmetric SMs [32] have also been shown to be possible.

Strictly speaking, the SM is not entirely a satisfactory model of particle phenomenology any longer, even apart from the hierarchy problem: it fails to explain neutrino oscillations; it does not contain good candidates for the dark matter; the generation of the baryon asymmetry in the electroweak phase transition is known to be problematic. Among the simplest extensions of the SM that can solve all these problems is the supersymmetric extension of the seesaw model [33]. In Ref. [34] we proposed a new scenario of inflation within the supersymmetric seesaw model, inspired by the developments of the nonminimally coupled

*masato.arai@fukushima-nct.ac.jp
†kawai@skku.edu
‡okadan@ua.edu

Higgs inflation models. Notably, in that scenario the problem associated with the large nonminimal coupling is alleviated. The purpose of the present paper is to discuss the viability of this inflationary scenario using realistic neutrino mass parameters. We follow the minimalistic guiding principle of Higgs inflation and consider the *minimal* seesaw model [35], i.e., with two families of the right-handed neutrinos. There are several other inflationary scenarios based on the supersymmetric seesaw model [36–42]. We shall compare the cosmological predictions of these models with ours, and argue that at least some of these models are soon to be excluded by CMB observations.

The main question we shall address below is whether or not the model allows parameter regions that are consistent with the observed baryon asymmetry, the spectrum of the CMB and the neutrino oscillation data. The ratio of the baryon density n_B to the entropy density s is measured to be [4,5]

$$Y_B \equiv \frac{n_B}{s} = 8.7 \times 10^{-11}. \tag{1}$$

As mentioned above, the electroweak baryogenesis within the SM is problematic as it requires rather implausible strongly first order electroweak phase transition. We show that in our scenario the thermal leptogenesis [43] with the reheating temperature $T_{\rm RH} \approx 10^5$ GeV, combined with the resonant enhancement effects [44–46] yields the observed amount of the baryon asymmetry (1). An interesting feature of our scenario is that the CMB spectrum is related to the seesaw mass scale [34]. We investigate this relation in the supersymmetric minimal seesaw model, and show that for a wide range of parameters our scenario is consistent with the present CMB observation. In the near future the CMB data will further constrain the seesaw mass scale. In our scenario the R-parity needs to be broken. We discuss that this requirement leads to a scenario of gravitino dark matter.

The paper is organized as follows. In the next section we describe the supersymmetric minimal seesaw model on which our scenario is based. In Sec. III the dynamics of inflation is discussed, and in Sec. IV the reheating process and baryogenesis are studied. The relation between the cosmological parameters and the neutrino mass parameters is discussed in Sec. V. Section VI deals with the R-parity violation. We conclude in Sec. VII with comments. Technicalities in computing the baryon asymmetry are relegated to the Appendix.

II. THE SUPERSYMMETRIC MINIMAL SEESAW MODEL

Our model is based on the supersymmetric seesaw model, with the superpotential,

$$W = \mu H_u H_d + y_u^{ij} u_i^c Q_j H_u + y_d^{ij} d_i^c Q_j H_d + y_e^{ij} e_i^c L_j H_d + y_D^{mi} N_m^c L_i H_u + \frac{1}{2} M_m N_m^c N_m^c. \tag{2}$$

Here, Q, u^c, d^c, L, e^c, H_u, H_d are the MSSM superfields, N_m^c the right-handed neutrino superfields (having odd R-parity), M_m the corresponding right-handed neutrino mass parameters, μ the MSSM μ-parameter and y_D^{mj}, y_u^{ij}, y_d^{ij}, y_e^{ij} are the Yukawa couplings. The superfields Q, L, H_u, H_d are $SU(2)$ doublets and the contraction using the $SU(2)$ invariant

$$i\sigma_2 = \begin{pmatrix} 0 & 1 \\ -1 & 0 \end{pmatrix}$$

is implicit, whereas u^c, d^c, e^c are $SU(2)$ singlets. In this paper we shall focus on the simplest realistic seesaw model with two right-handed neutrinos (the minimal seesaw model [35]). Thus the family indices run $m, n, \ldots = 1, 2$ for the right-handed neutrinos and $i, j, \ldots = 1, 2, 3$ for the other lepton and the quark superfields.

Using the stationarity condition $\delta W/\delta N_m^c = y_D^{mi} L_i H_u + M_m N_m^c = 0$, the superpotential along the flat direction reads

$$W_{\rm eff} = N_m^c (y_D^{mi} L_i H_u + M_m N_m^c) - \frac{1}{2} M_m N_m^c N_m^c = -\frac{1}{2} M_m^{-1} (y_D^{mi} L_i H_u)(y_D^{mj} L_j H_u). \tag{3}$$

The Higgs field develops the vacuum expectation value at low energies,

$$\langle H_u \rangle = \begin{pmatrix} 0 \\ \langle H_u^0 \rangle \end{pmatrix}, \tag{4}$$

where $\langle H_u^0 \rangle = \frac{v}{\sqrt{2}} \sin\beta$ with $v = 246$ GeV. We use $\tan\beta = 10$ throughout this paper. The mass matrix of the left-handed neutrinos obtained from (3) is

$$m_\nu = m_D^T M^{-1} m_D, \tag{5}$$

where $m_D = y_D \langle H_u^0 \rangle$ and $M = \mathrm{diag}(M_1, M_2)$. This is the celebrated seesaw relation. The Maki-Nakagawa-Sakata (MNS) lepton flavor mixing matrix is parametrized as

$$U_{\rm MNS} = \begin{pmatrix} c_{12}c_{13} & s_{12}c_{13} & s_{13}e^{-i\delta} \\ -s_{12}c_{23} - c_{12}s_{23}s_{13}e^{i\delta} & c_{12}c_{23} - s_{12}s_{23}s_{13}e^{i\delta} & s_{23}c_{13} \\ s_{12}s_{23} - c_{12}c_{23}s_{13}e^{i\delta} & -c_{12}s_{23} - s_{12}c_{23}s_{13}e^{i\delta} & c_{23}c_{13} \end{pmatrix} \begin{pmatrix} 1 & 0 & 0 \\ 0 & e^{i\sigma} & 0 \\ 0 & 0 & 1 \end{pmatrix}, \tag{6}$$

where $s_{ij} = \sin\theta_{ij}$, $c_{ij} = \cos\theta_{ij}$, and δ, σ are the CP-violating Dirac and Majorana phases. The neutrino mass matrix is diagonalized by the MNS matrix as

$$m_\nu = U^*_{\rm MNS} D_\nu U^\dagger_{\rm MNS}, \tag{7}$$

where $D_\nu \equiv \mathrm{diag}(m_1, m_2, m_3)$. We use the neutrino mass parameters from the oscillation data [47,48],

$$\sin^2 2\theta_{12} = 0.87, \quad \sin^2 2\theta_{23} = 1.0,$$
$$\sin^2 2\theta_{13} = 0.092, \quad \Delta m^2_{12} \equiv m_2^2 - m_1^2 = 7.59 \times 10^{-5}\ \mathrm{eV}^2,$$
$$\Delta m^2_{23} \equiv |m_3^2 - m_2^2| = 2.43 \times 10^{-3}\ \mathrm{eV}^2. \tag{8}$$

In terms of these the neutrino masses are

$$m_1 = 0, \quad m_2 = \sqrt{\Delta m^2_{12}}, \quad m_3 = \sqrt{\Delta m^2_{12} + \Delta m^2_{23}}, \tag{9}$$

for the normal mass hierarchy (NH) and

$$m_1 = \sqrt{\Delta m^2_{23} - \Delta m^2_{12}}, \quad m_2 = \sqrt{\Delta m^2_{23}}, \quad m_3 = 0, \tag{10}$$

for the inverted mass hierarchy (IH). The neutrino mass matrix can be conveniently parametrized as [49,50]

$$m_D = \sqrt{M} R \sqrt{D_\nu} U^\dagger_{\rm MNS}, \tag{11}$$

where $\sqrt{M} \equiv \mathrm{diag}(\sqrt{M_1}, \sqrt{M_2})$ and

$$\sqrt{D_\nu} = \begin{cases} \sqrt{D_\nu^{\rm NH}} = \begin{pmatrix} 0 & \sqrt{m_2} & 0 \\ 0 & 0 & \sqrt{m_3} \end{pmatrix}, \\ \sqrt{D_\nu^{\rm IH}} = \begin{pmatrix} \sqrt{m_1} & 0 & 0 \\ 0 & \sqrt{m_2} & 0 \end{pmatrix}. \end{cases} \tag{12}$$

In (11), R is a 2×2 orthogonal matrix

$$R = \begin{pmatrix} \cos w & \sin w \\ -\sin w & \cos w \end{pmatrix}, \quad w \in \mathbb{C}. \tag{13}$$

We shall write the real and imaginary parts of w as $w = a + ib$, $a, b \in \mathbb{R}$. A merit of the minimal seesaw model is its strong predictive power. Note that the mass matrix m_D (or equivalently the Dirac Yukawa coupling y_D) contains 9 real degrees of freedom (6 complex minus 3 phases), 5 of which are constrained by the oscillation data, namely the two neutrino masses and the three angles in (8). In addition, there are one Dirac and one Majorana phases, and the remaining two degrees of freedom correspond to the choice of a and b. The right-handed neutrino masses M_1, M_2 and the Dirac and Majorana phases are not fixed by the present experiments. In our scenario these parameters are subject to the constraints from the CMB, as discussed below.

III. INFLATIONARY DYNAMICS AND COSMOLOGICAL PARAMETERS

In this section we describe the construction of the inflation model and discuss its prediction on cosmological parameters. The model, which is a multi-family generalization of the one introduced in Ref. [34], has some similarity to the supersymmetric Higgs inflation models [27–30]. A notable difference from these models is that the nonminimal coupling ξ is allowed to take small values and the unitarity violation problem is thus alleviated.

A. The model of inflation

We assume that inflation takes place along one of the L-H_u D-flat directions and as an initial condition one of the three (scalar components of the) L_i fields, call it L_k with k fixed, has a large expectation value and dominates the inflationary dynamics over the other L_i's. The D-flat direction along L_k-H_u can be parametrized as

$$L_k = \frac{1}{\sqrt{2}} \begin{pmatrix} \varphi \\ 0 \end{pmatrix}, \quad H_u = \frac{1}{\sqrt{2}} \begin{pmatrix} 0 \\ \varphi \end{pmatrix}, \tag{14}$$

with k fixed. Disregarding Q, u^c, d^c, e^c, H_d that play no role during inflation, the superpotential (2) reads

$$W_{\rm inf} = \frac{1}{2} y_D^{mk} N^c_m \varphi^2 + \frac{1}{2} M_m N^c_m N^c_m. \tag{15}$$

For the Kähler potential $K \equiv -3\Phi$ we choose a slightly noncanonical form,

$$\begin{aligned} \Phi &= 1 - \frac{1}{3}(|L_k|^2 + |H_u|^2 + |N^c_1|^2 + |N^c_2|^2) \\ &\quad + \frac{\gamma}{2}(L_k H_u + \mathrm{c.c.}) + \frac{\zeta}{3}(|N^c_1|^4 + |N^c_2|^4) \\ &= 1 - \frac{1}{3}(|\varphi|^2 + |N^c_1|^2 + |N^c_2|^2) + \frac{\gamma}{4}(\varphi^2 + \bar\varphi^2) \\ &\quad + \frac{\zeta}{3}(|N^c_1|^4 + |N^c_2|^4). \end{aligned} \tag{16}$$

The terms proportional to γ yield nonminimal coupling between the inflaton and the background curvature, and the other noncanonical terms proportional to ζ have been introduced for controlling the inflaton trajectory. The supergravity scalar potential (in the Jordan frame) is computed from (15) and (16) as (see Ref. [51]),

$$\begin{aligned} V_F &= |y_D^{nk} N^c_n \varphi|^2 + A_1 \\ &\quad - \frac{|y_D^{nk} N^c_n (\varphi^2 - \frac{3}{2}\gamma|\varphi|^2) + A_2 - 3W_{\rm inf}|^2}{3 - \frac{3}{4}\gamma(\varphi^2 + \bar\varphi^2) + \frac{9}{4}\gamma^2|\varphi|^2 + A_3}, \end{aligned} \tag{17}$$

where the repeated n's are summed over, k is fixed (no sum), and

$$\begin{aligned} A_1 &= \sum_{m=1,2} \frac{|\frac{1}{2} y_D^{mk} \varphi^2 + M_m N^c_m|^2}{1 - 4\zeta|N^c_m|^2}, \\ A_2 &= \sum_{m=1,2} \frac{(\frac{1}{2} y_D^{mk} \varphi^2 + M_m N^c_m) N^c_m (1 - 2\zeta|N^c_m|^2)}{1 - 4\zeta|N^c_m|^2}, \\ A_3 &= \sum_{m=1,2} \frac{\zeta|N^c_m|^4}{1 - 4\zeta|N^c_m|^2}. \end{aligned} \tag{18}$$

The Dirac Yukawa coupling is

$$y_D = \frac{\sqrt{2}}{v \sin\beta} \sqrt{M} R \sqrt{D_\nu} U_{\rm MNS}^\dagger, \tag{19}$$

and in (17) the fields φ and N_m^c are understood to be the scalar components. In the Einstein frame the scalar potential is

$$V_{\rm E} = \frac{V_F}{\Phi^2}. \tag{20}$$

B. The inflaton trajectory

The model of inflation we consider is a system of three complex scalar fields φ, N_1^c and N_2^c. While the dynamics could consequently be quite involved in general, it turns out that under mild assumptions the model reduces to that of single-field slow roll inflation. This is by virtue of the noncanonical terms in the Kähler potential proportional to ζ.

When M_m are large our model is similar to the supersymmetric versions of SM Higgs inflation discussed in Refs. [27–30]. Let us consider, as an example, the seesaw masses $M_1 = M_2 = 10^{13}$ GeV and choose for concreteness the normal mass hierarchy of the neutrinos and $a = 0$, $b = 1$, $\delta = 0$, $\sigma = 0$. Then the Yukawa coupling are found to be

$$\begin{aligned} y_D^{11} &= 0.0465 + 0.0233i, & y_D^{21} &= 0.0306 - 0.0354i, \\ y_D^{12} &= 0.0434 + 0.106i, & y_D^{22} &= 0.139 - 0.0331i, \\ y_D^{13} &= -0.0536 + 0.106i, & y_D^{23} &= 0.139 + 0.0408i. \end{aligned} \tag{21}$$

The dynamics of inflation can be studied by examining the steepest descent trajectory of the scalar potential (20). Assuming that inflation takes place in the L_k-H_u D-flat direction along the first generation lepton supermultiplet ($k = 1$) and the e-folding number $N_e = 60$, we find $\xi = 1674$ fixed by the CMB power spectrum (procedure explained in the next subsection). It is found numerically that the trajectory is along ${\rm Im}\varphi = 0$. We thus consider only the real values of φ. The inflaton trajectory fluctuates in the directions of N_m^c as shown in Fig. 1, where the values of the real and imaginary parts of N_1^c and N_2^c are plotted along the steepest descent trajectory. The parameter ζ for the quartic terms in the Kähler potential is chosen to be a moderate value[1] $\zeta = 100$ and the field values are measured in the reduced Planck unit $8\pi G = 1$. While the trajectory seems rather complicated, inflation actually terminates [that is, one of the slow roll parameters becomes $\mathcal{O}(1)$] before the complication starts. In the example considered

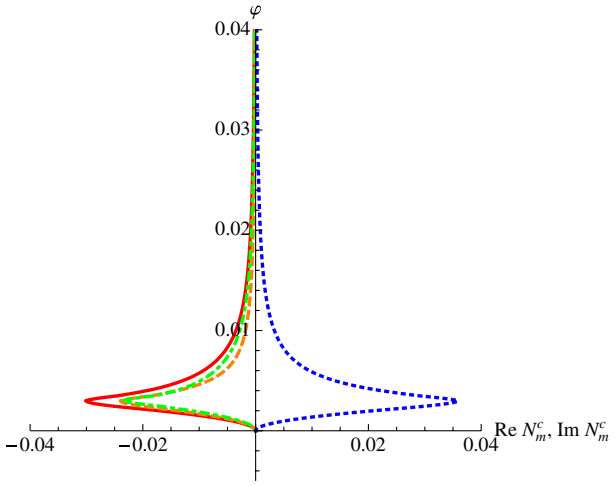

FIG. 1 (color online). The steepest descent trajectory of the scalar potential (20), for $M_1 = M_2 = 10^{13}$ GeV, $a = 0$, $b = 1$, $\delta = 0$, $\sigma = 0$ and $k = 1$, $\xi = 1674$, $\zeta = 100$. The red solid, the orange dashed, the green dot-dashed and the blue dotted curves respectively shows the values of ${\rm Re}N_1^c$, ${\rm Im}N_1^c$, ${\rm Re}N_2^c$ and ${\rm Im}N_2^c$. The slow roll terminates at $\varphi = 0.0371$. The field values are measured in the reduced Planck unit $8\pi G = 1$.

here the slow roll terminates at $\varphi = 0.0371$, where N_1^c and N_2^c are still stabilized close to $N_m^c = 0$. Figure 2 shows the shape of the potential as a function of φ and ${\rm Re}N_1^c$, where ${\rm Im}N_1^c$, ${\rm Re}N_2^c$, ${\rm Im}N_2^c$ are taken to be along the trajectory of Fig. 1. In this case[2] the primordial tilt and the tensor-to-scalar ratio of the CMB are computed to be $n_s = 0.968$, $r = 0.00296$. The red spectrum with very small r is typical of the nonminimally coupled Higgs inflation. The horizon exit of the comoving CMB scale takes place at $\varphi = 0.318$. In computing the CMB spectrum the role played by ζ is minor, as ζ has no effects once the inflaton trajectory is stabilized along $N_m^c \approx 0$.

Setting N_1^c, $N_2^c \to 0$ and restricting φ to take real values, the scalar potential (17) simplifies to

$$V_F = \frac{\lambda}{4}\varphi^4, \tag{22}$$

where $\lambda \equiv (y_D^\dagger y_D)_{kk}$ is the k-k component ($k = 1, 2, 3$) of the matrix representation of

$$y_D^\dagger y_D = \frac{2}{v^2 \sin^2\beta} U_{\rm MNS} \sqrt{D_\nu}^T R^\dagger M R \sqrt{D_\nu} U_{\rm MNS}^\dagger. \tag{23}$$

The resulting inflationary model is essentially the nonminimally coupled $\lambda\phi^4$ model, discussed in Ref. [52]. We have analyzed the above example (corresponding to $\lambda = (y_D^\dagger y_D)_{11} = 0.00490$) in this approximation, and found essentially no difference. For example the predictions for n_s and r are exactly the same within 3 significant

[1]Being higher order terms in the Kähler potential, ζ is expected to be not much larger than ξ. For zero or small ζ the multi-field effects become important. While the physics of the isocurvature modes and non-Gaussianity arising in the small ζ case would also be of interest, we shall not discuss such issues in this paper.

[2]In deriving these values the deviation from N_1^c, $N_2^c = 0$ are taken into account but the dynamics of N_m^c are neglected.

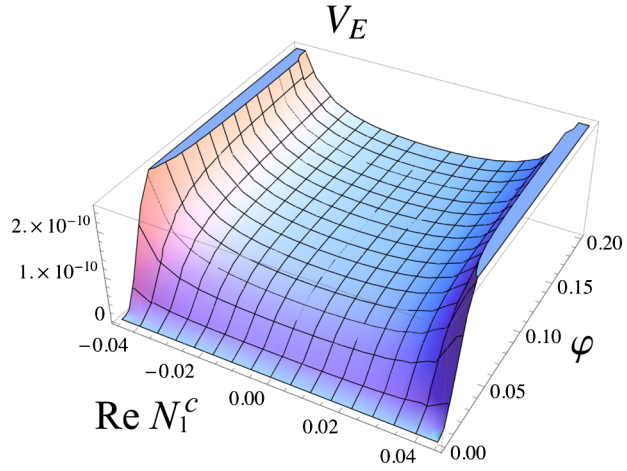

FIG. 2 (color online). The scalar potential $V_{\rm E}$ as a function of φ and $\mathrm{Re}N_1^c$. The other fields $\mathrm{Im}N_1^c$, $\mathrm{Re}N_2^c$, $\mathrm{Im}N_2^c$ are chosen to take values along the steepest descent trajectory.

digits. For smaller M_m the effects of nonzero N_m^c become even more negligible, as the slow roll terminates at a larger value of φ and the turn around behavior of N_m^c occurs at the smaller mass scale of M_m.

C. Cosmological parameters

As the single field approximation $N_m^c = 0$, $\varphi \in \mathbb{R}$ is sufficiently accurate, we shall study the inflationary dynamics within this approximation. We rescale the inflaton field as

$$\chi = \sqrt{2}\varphi, \tag{24}$$

so that the kinetic term is canonically normalized in the Lagrangian

$$\mathcal{L}_{\rm J} = \sqrt{-g_{\rm J}}\left[\frac{1+\xi\chi^2}{2}R_{\rm J} - \frac{1}{2}g_{\rm J}^{\mu\nu}\partial_\mu\chi\partial_\nu\chi - V_F\right]. \tag{25}$$

Here the subscript J indicates the Jordan frame and

$$V_F = \frac{\lambda}{16}\chi^4, \qquad \xi \equiv \frac{\gamma}{4} - \frac{1}{6}. \tag{26}$$

This is the Lagrangian in the Jordan frame where the scalar field is nonminimally coupled to the background curvature. The Lagrangian in the Einstein frame is obtained by the Weyl transformation $g^{\rm E}_{\mu\nu} = (1+\xi\chi^2)g^{\rm J}_{\mu\nu}$. The canonically normalized inflaton field $\hat{\chi}$ in the Einstein frame is related to χ by

$$d\hat{\chi} = \frac{\sqrt{1+\xi\chi^2+6\xi^2\chi^2}}{1+\xi\chi^2}d\chi. \tag{27}$$

The potential in the Einstein frame is

$$V_{\rm E} = \frac{\lambda}{16}\frac{\chi^4}{1+\xi\chi^2}, \tag{28}$$

in terms of which the slow roll parameters in the Einstein frame are defined as

$$\epsilon = \frac{1}{2}\left(\frac{1}{V_{\rm E}}\frac{dV_{\rm E}}{d\hat{\chi}}\right)^2, \qquad \eta = \frac{1}{V_{\rm E}}\frac{d^2V_{\rm E}}{d\hat{\chi}^2}. \tag{29}$$

The potential $V_{\rm E}$ in the single field approximation (28) is much simpler than the original one (17) and is determined solely by $\lambda = (y_D^\dagger y_D)_{kk}$ and ξ. For given λ and the e-folding number N_e, the nonminimal coupling ξ is fixed by the CMB power spectrum. For definiteness we use the maximum likelihood value $\Delta_R^2(k_0) = 2.43\times10^{-9}$ from the 9-year Wilkinson Microwave Anisotropy Probe data [4,5], where the calibration is set at $k_0 = 0.002\ \mathrm{Mpc}^{-1}$. This is related to the power spectrum $\mathcal{P}_R = V_{\rm E}/24\pi^2\epsilon$ of the curvature perturbation (at the horizon exit of the comoving scale) by $\Delta_R^2(k) = \frac{k^3}{2\pi^2}\mathcal{P}_R(k)$. We denote the value of χ at the end of the slow roll (characterized by $\max(\epsilon,\eta) = 1$) as $\chi = \chi_*$, and the value of χ at the horizon exit of the comoving CMB scale k as $\chi = \chi_k$. These are related by the e-folding number through $N_e = \int_{\chi_*}^{\chi_k} d\chi V_{\rm E}(d\hat{\chi}/d\chi)/(dV_{\rm E}/d\hat{\chi})$.

From the values of the slow roll parameters at the horizon exit of the comoving CMB scale, the scalar spectral index $n_s \equiv d\ln\mathcal{P}_R/d\ln k = 1-6\epsilon+2\eta$ and the tensor-to-scalar ratio $r \equiv \mathcal{P}_{\rm gw}/\mathcal{P}_{\rm R} = 16\epsilon$ can be computed. The results[3] are summarized in Table I, for $N_e = 50$, 60 and several values of $\lambda = (y_D^\dagger y_D)_{kk}$. There exists a lower bound on λ set by the minimal coupling limit $\xi \to 0$. In this limit the model reduces to chaotic inflation with the quartic potential $V_{\rm E} = \frac{\lambda}{16}\chi^4$, where $\lambda = 1.05\times10^{-12}$ for $N_e = 50$ and $\lambda = 6.19\times10^{-13}$ for $N_e = 60$, fixed by the value of $\mathcal{P}_R$. In contrast to the SM [6–19] and the supersymmetric [27–30] Higgs inflation models the nonminimal coupling ξ does not need to be large. We see from the table that $\xi \lesssim \mathcal{O}(1)$ for $\lambda \lesssim 10^{-9}$. Hence, at least for these values of λ the model is obviously free from the danger of violating the unitarity bound. Small ξ is also favored for avoiding large R-parity violation, as discussed later in Sec. VI. The Dirac Yukawa coupling y_D^{mi} is related to a, b, δ, σ, M_1, M_2 through (19). We will discuss the relation between λ and these parameters in Sec. V. Leptogenesis also constrains certain neutrino mass parameters, which will be discussed in Sec. IV.

D. Observational constraints and comparison with other models based on supersymmetric seesaw

We show in Fig. 3 the predicted values of n_s and r of our model along with the 68% and 95% confidence level contours from the WMAP9 + eCMB + BAO + H_0 data [4,5]. The prediction is seen to be consistent with the

[3]These are the results of the tree-level computation. The renormalization effects are verified to be negligibly small [30,34].

TABLE I. The nonminimal coupling ξ, the inflaton values at the end of the slow roll (χ_*) and at the horizon exit (χ_k), the spectral index n_s, and the tensor-to-scalar ratio r for e-folding $N_e = 50$, 60 and for various different values of $\lambda = (y_D^\dagger y_D)_{kk}$. The coupling ξ is fixed by the amplitude of the curvature perturbation. The last lines ($N_e = 50$, $\lambda = 1.05 \times 10^{-12}$ and $N_e = 60$, $\lambda = 6.19 \times 10^{-13}$) correspond to minimal coupling.

N_e	$\lambda \equiv (y_D^\dagger y_D)_{kk}$	ξ	χ_*	χ_k	n_s	r
	0.1	6348	0.0135	0.106	0.962	0.00419
	10^{-3}	635	0.0426	0.335	0.962	0.00419
	10^{-5}	63.4	0.135	1.06	0.962	0.00420
	10^{-7}	6.26	0.424	3.33	0.962	0.00430
50	10^{-9}	0.555	1.28	9.94	0.961	0.00545
	10^{-10}	0.131	2.02	15.4	0.961	0.00945
	10^{-11}	0.0188	2.99	19.5	0.959	0.0379
	5×10^{-12}	8.70×10^{-3}	3.21	20.0	0.957	0.0691
	2×10^{-12}	2.15×10^{-3}	3.39	20.2	0.951	0.165
	1.05×10^{-12}	0	3.46	20.3	0.942	0.311
	0.1	7567	0.0124	0.106	0.968	0.00296
	10^{-3}	757	0.0391	0.335	0.968	0.00296
	10^{-5}	75.6	0.123	1.06	0.968	0.00297
	10^{-7}	7.48	0.389	3.33	0.968	0.00303
	10^{-9}	0.676	1.18	10.0	0.968	0.00369
60	10^{-10}	0.168	1.90	15.9	0.968	0.00588
	10^{-11}	0.0270	2.84	20.8	0.966	0.0203
	5×10^{-12}	0.0135	3.10	21.5	0.965	0.0356
	2×10^{-12}	4.44×10^{-3}	3.32	22.0	0.962	0.0822
	10^{-12}	1.24×10^{-3}	3.42	22.2	0.957	0.161
	6.19×10^{-13}	0	3.46	22.2	0.951	0.260

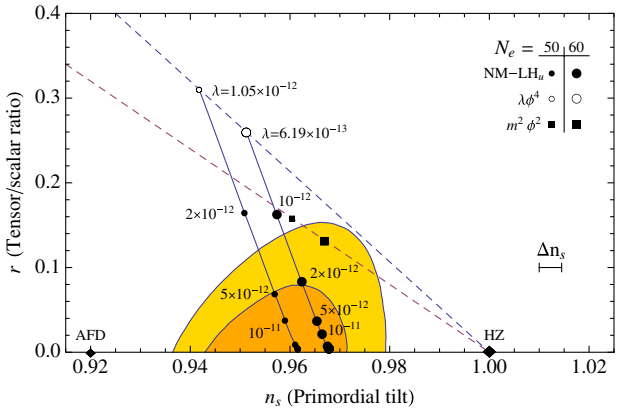

FIG. 3 (color online). Plot of the scalar spectral index n_s and the tensor-to-scalar ratio r, with the 68% and 95% confidence level contours from the WMAP9 + eCMB + BAO + H_0 data [4,5]. Indicated by • are the prediction of our model (NM-LH_u) for e-folding numbers $N_e = 50$ and 60. The coupling $\lambda = (y_D^\dagger y_D)_{kk}$ is a diagonal element of (23), which is related to the neutrino mass parameters (see Sec. V). For comparison, the spectra of the Harrison-Zel'dovich (HZ), the $m^2\phi^2$ minimally coupled chaotic inflation model, as well as the A-term-lifted MSSM flat-direction inflation model (AFD) are also indicated. Δn_s is the expected Planck accuracy [54,55].

present data, apart from the regions where the Yukawa coupling is extremely small. The 2-σ constraints roughly correspond to $M_m \gtrsim$ TeV, details of which depending on the other neutrino mass parameters (see Sec. V). While the minimally coupled $\lambda\phi^4$ model lies outside the 2-σ constraints, the nonminimally coupled $\lambda\phi^4$, even if the coupling is as small as $\xi \sim 10^{-2}$, sits well inside the 1-σ constraints. In the figure we also indicate for comparison the Harrison-Zel'dovich spectrum as well as the spectra of two other inflationary models arising from the supersymmetric seesaw model. These are:

$\tilde{N}_R$ chaotic inflation model—Inflation is driven by a right-handed scalar neutrino, with the seesaw mass scale identified as the inflaton mass [36–38]. It is essentially the minimally coupled $m^2\phi^2$ chaotic inflation model, but has phenomenological advantages such as automatic leptogenesis. The spectrum is marked with ■ in the figure.

A-term inflation model—This model assumes $u^c d^c d^c$, $e^c LL$, or $N_R^c L H_u$ direction of the (singlet-extended) MSSM as the inflaton [39–42]. The A-term inflation model predicts very small r and $n_s \approx 1$–$4/N_e$. Since inflation takes place at a low energy scale and the e-folding cannot be large ($N_e \lesssim 50$), we show the case for $N_e = 50$ (thus $n_s = 0.92$) in the figure, marked with ◆ (AFD).[4] In the figure we also indicate the expected resolution $\Delta n_s \approx 0.0045$ of the Planck satellite experiments [54,55]. The data from the Planck satellite is soon to be available. There are more sensitive CMB polarization experiments planned in the near future [56,57], which we expect will put these models to the test with even higher resolution.

IV. REHEATING AND BARYOGENESIS

The scalar potential (20) has a minimum at $\varphi = N_m^c = 0$ corresponding to the global supersymmetric vacuum. After the slow roll, the inflaton undergoes coherent oscillations about this minimum and decays into the SM particles, followed by thermalization. The nonminimal coupling can alter the reheating temperature only when ξ is extremely large and the decay rate is very small [58,59]. In the model we are discussing the inflaton is in the L-H_u direction and the coupling to the SM particles is not small. The nonminimal coupling thus has negligible effects on the reheating process. The upper bound of the reheating temperature can be estimated as $T_{\rm RH} \lesssim 10^7$ GeV, assuming the Higgs component decay channel $\varphi \to b\bar{b}$ in the conservative perturbative decay scenario. The nonperturbative reheating scenario [60] (with parametric resonance) and/or the (s)lepton component decay may lead to a slightly higher upper bound. Taking into account the effects of the redshift during the time needed for thermalization,

[4]There exists a variant of A-term inflation, called inflection point inflation [53] While this model allows $n_s \geq 0.92$, it has less predictive power on the spectrum.

we estimate the reheating temperature of this scenario to be $T_{\rm RH} \approx 10^5$–10^7 GeV. Below in this section we discuss implication of this reheating temperature on the generation of the baryon asymmetry. The constraints from the R-parity violation will be discussed in Sec. VI.

The baryon asymmetry (1) can be accounted for by different mechanisms, depending on the seesaw mass scale M_m. If the mass scale is smaller than the reheating temperature $M_m \lesssim T_{\rm RH}$, the right-handed (s)neutrinos thermalize and their decay generates lepton number asymmetry. The lepton number is later converted into the baryon number through the sphaleron process. This mechanism is known as thermal leptogenesis [43]. If the seesaw mass scale is larger than the reheating temperature $M_m \gtrsim T_{\rm RH}$, on the other hand, the lepton number can be generated by the decay of oscillating sneutrinos [36,37,61]. We call this mechanism nonthermal leptogenesis. The generated lepton number is converted into the baryon number, similarly to the thermal leptogenesis case. In addition, as our model includes the MSSM components, the Affleck-Dine mechanism [62] can be operative. We shall discuss the thermal and the nonthermal leptogenesis in our model below.

A. Thermal leptogenesis

In the leptogenesis scenario the out-of-equilibrium decay of the right-handed (s)neutrinos generates the lepton asymmetry, which is later converted into the baryon asymmetry by the $(B+L)$-violating sphaleron transitions. In the supersymmetric theory the conversion rate is computed to be

$$Y_B = -\frac{8N_f + 4N_H}{22N_f + 13N_H} Y_L = -\frac{8}{23} Y_L, \tag{30}$$

where Y_L is the yield (the ratio of the number density to the entropy density) of the leptons, and $N_f = 3, N_H = 2$ are the number of the fermion families and the number of the Higgs doublets.

In generic scenarios of leptogenesis, generation of sufficient baryon asymmetry requires the reheating temperature to be higher than 10^9 GeV. This is much higher than the reheating temperature of our scenario, and in supersymmetric models the gravitino problem can also be serious. It has been pointed out, however, that if the two right-handed neutrino masses are nearly degenerate the CP-asymmetry parameter is enhanced by resonance effects, making the leptogenesis viable even at lower reheating temperature [44–46]. In the following we assume the resonant leptogenesis scenario with nearly degenerate right-handed neutrino masses $M_1 \approx M_2$. Thermalization of the right-handed neutrinos after reheating also requires $M_1, M_2 \lesssim T_{\rm RH}$.

The decay modes of the right-handed (s)neutrinos are

$$\begin{aligned} &N_m \to \tilde{\ell}_j + \bar{\tilde{h}}, \qquad N_m \to \ell_j + H_u, \\ &\widetilde{N}^c_m \to \tilde{\ell}_j + H_u, \qquad \widetilde{N}^{c\,\dagger}_m \to \ell_j + \bar{\tilde{h}}, \end{aligned} \tag{31}$$

and the CP-asymmetry parameters associated with these processes are defined as

$$\begin{aligned} \varepsilon_m &\equiv \frac{\sum_j[\Gamma(N_m \to \tilde{\ell}_j + \bar{\tilde{h}}) - \Gamma(N_m \to \tilde{\ell}^\dagger_j + \tilde{h})]}{\sum_j[\Gamma(N_m \to \tilde{\ell}_j + \bar{\tilde{h}}) + \Gamma(N_m \to \tilde{\ell}^\dagger_j + \tilde{h})]} \\ &= \frac{\sum_j[\Gamma(N_m \to \ell_j + H_u) - \Gamma(N_m \to \tilde{\ell}_j + H^\dagger_u)]}{\sum_j[\Gamma(N_m \to \ell_j + H_u) + \Gamma(N_m \to \tilde{\ell}_j + H^\dagger_u)]} \\ &= \frac{\sum_j[\Gamma(\widetilde{N}^c_m \to \tilde{\ell}_j + H_u) - \Gamma(\widetilde{N}^{c\,\dagger}_m \to \tilde{\ell}^\dagger_j + H^\dagger_u)]}{\sum_j[\Gamma(\widetilde{N}^c_m \to \tilde{\ell}_j + H_u) + \Gamma(\widetilde{N}^{c\,\dagger}_m \to \tilde{\ell}^\dagger_j + H^\dagger_u)]} \\ &= \frac{\sum_j[\Gamma(\widetilde{N}^{c\,\dagger}_m \to \ell_j + \bar{\tilde{h}}) - \Gamma(\widetilde{N}^c_m \to \bar{\ell}_j + \tilde{h})]}{\sum_j[\Gamma(\widetilde{N}^{c\,\dagger}_m \to \ell_j + \bar{\tilde{h}}) + \Gamma(\widetilde{N}^c_m \to \bar{\ell}_j + \tilde{h})]}. \end{aligned} \tag{32}$$

Here, $\widetilde{N}^c_m$ denotes the right-handed scalar neutrinos, $\tilde{h}$ denotes the (up-type) higgsinos, and ℓ, $\tilde{\ell}$ are the components of the lepton and scalar lepton doublets. We follow the notation of Plumacher [63]. The CP asymmetry parameters are computed from the interference of the tree and one-loop diagrams. In Fig. 4 we show the diagrams contributing to one of the decay modes $N_m \to \tilde{\ell}_j + \bar{\tilde{h}}$. The resulting formula for the CP-asymmetry parameters is

$$\varepsilon_m \equiv \sum_{n \neq m} \frac{-{\rm Im}[(y_D y_D^\dagger)^2_{mn}]}{(y_D y_D^\dagger)_{mm}(y_D y_D^\dagger)_{nn}} \frac{M_m \Gamma_n}{M_n^2} \left(\frac{1}{2} V_n + S_n\right), \tag{33}$$

where $\Delta M^2_{mn} = M^2_m - M^2_n$, and

$$V_n = \frac{M_n^2}{M_m^2} \ln\left(1 + \frac{M_m^2}{M_n^2}\right), \tag{34}$$

$$S_n = \frac{M_n^2 \Delta M^2_{nm}}{(\Delta M^2_{nm})^2 + M_m^2 \Gamma_n^2}, \tag{35}$$

corresponding respectively to the vertex corrections (such as the 2nd and 3rd diagrams of Fig. 4) and the self-energy

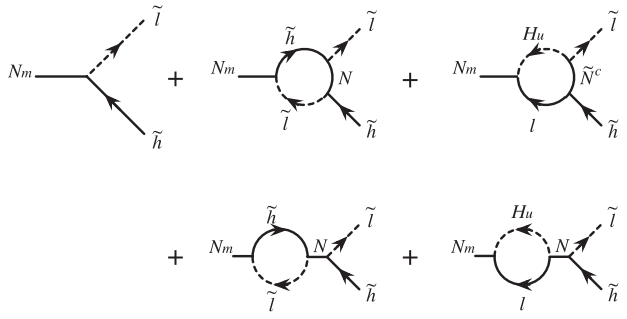

FIG. 4. The diagrams contributing to the decay mode $N_m \to \tilde{\ell} + \bar{\tilde{h}}$.

corrections (the 4th and 5th diagrams). The decay width is written as

$$\Gamma_n = \frac{(y_D y_D^\dagger)_{nn}}{4\pi} M_n. \tag{36}$$

The lepton asymmetry Y_L, and hence the baryon asymmetry through the conversion (30), are found by solving the Boltzmann equations. We summarize the Boltzmann equations and related formulas in the Appendix. Here we discuss the results and features that are relevant to our model. We first notice that the CP phases δ and σ do not affect the baryon asymmetry. This is due to the fact that the MNS matrices cancel in the product of the Yukawa couplings appearing in (33),

$$y_D y_D^\dagger = \frac{2}{v^2 \sin^2\beta} \sqrt{M} R \tilde{D}_\nu R^\dagger \sqrt{M}. \tag{37}$$

Here, $\tilde{D}_\nu = \mathrm{diag}(m_2, m_3)$ for the normal mass hierarchy and $\tilde{D}_\nu = \mathrm{diag}(m_1, m_2)$ for the inverted mass hierarchy. The baryon number, on the other hand, depends on the parameters a, b in (13), as well as on the right-handed neutrino masses M_1, M_2. In Fig. 5 we show the yield of the baryon asymmetry Y_B, as a and b are varied. The left panel shows the result for the normal mass hierarchy with $M_1 = 10^5$ GeV, and the right panel is for the inverted mass hierarchy with $M_1 = 10^7$ GeV. In both panels the mass difference is chosen to be $M_2 - M_1 = 10^{-7} \times M_1$. The red contour curves indicate $Y_B = 8.7 \times 10^{-11}$ corresponding to the observed value.

The dependence of the baryon asymmetry of the universe on these parameters can be understood as follows. The baryon asymmetry generated through thermal leptogenesis is proportional to the CP violation parameter ε_m as [64,65]

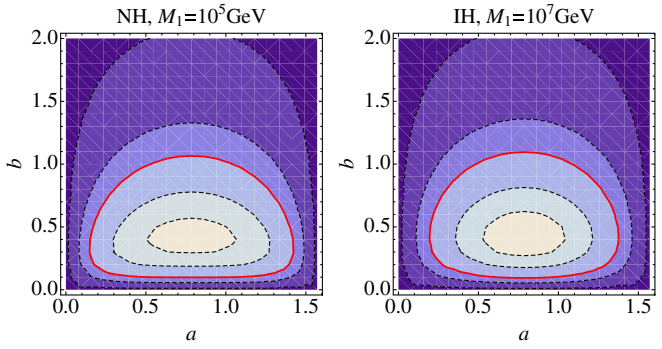

FIG. 5 (color online). The neutrino mass parameters a and b yielding the observed value of the baryon asymmetry $Y_B = 8.7 \times 10^{-11}$ (the red contour curves). The left panel shows the case $M_1 = 10^5$ GeV with the normal mass hierarchy, and the right panel is for $M_1 = 10^7$ GeV with the inverted mass hierarchy. In both panels the contours are $Y_B = 2 \times 10^{-10}$, 1.5×10^{-10}, 8.7×10^{-11}, 5×10^{-11}, 1×10^{-11} from inside. We have chosen $(M_2 - M_1)/M_1 = 10^{-7}$.

$$Y_B \approx \kappa \frac{\varepsilon_m}{g_*}, \tag{38}$$

where $g_* \approx 200$ is the number of degrees of freedom during leptogenesis and $\kappa \lesssim 1$ is the efficiency factor depending on details of the Boltzmann equations. In the resonant leptogenesis with nearly degenerate right-handed neutrino masses $M_1 \approx M_2$ we find $V_n \approx \ln 2 \ll S_n$. The maximal enhancement of the CP asymmetry parameter ε_m occurs when the decay width of either of the right-handed (s)neutrinos becomes close to the mass difference,[5] $\Delta M_{nm}^2 \approx M_m \Gamma_n$. Parametrizing the mass difference as $\Delta M_{21}^2 = \alpha M_1 \Gamma_2$, the CP asymmetry parameters read

$$\begin{aligned} \varepsilon_1 &\approx -\frac{\alpha}{1+\alpha^2} \frac{\mathrm{Im}[(y_D y_D^\dagger)_{12}^2]}{(y_D y_D^\dagger)_{11}(y_D y_D^\dagger)_{22}}, \\ \varepsilon_2 &\approx \frac{(\alpha^2+1)\Gamma_1\Gamma_2}{\Gamma_1^2 + \alpha^2\Gamma_2^2} \varepsilon_1. \end{aligned} \tag{39}$$

For the (nearly) degenerate right-handed neutrino masses, the matrix $\sqrt{M}$ in (37) becomes proportional to the identity. Then $\mathrm{Im}[(y_D y_D^\dagger)_{12}^2]/(y_D y_D^\dagger)_{11}(y_D y_D^\dagger)_{22}$ is written as

$$\frac{2(m_2^2 - m_3^2)\sin 2a \sinh 2b}{(m_2 - m_3)^2 \cos^2 2a - (m_2 + m_3)^2 \cosh^2 2b}, \tag{40}$$

for the normal mass hierarchy and

$$\frac{2(m_1^2 - m_2^2)\sin 2a \sinh 2b}{(m_1 - m_2)^2 \cos^2 2a - (m_1 + m_2)^2 \cosh^2 2b}, \tag{41}$$

for the inverted mass hierarchy. These have maxima at $a = \pi/4 \approx 0.785$ and $b = \ln(3 + 2\sqrt{2})/4 \approx 0.441$, with maximal value $(m_3 - m_2)/(m_3 + m_2) \approx 0.704$ for (40) and $(m_2 - m_1)/(m_2 + m_1) \approx 7.93 \times 10^{-3}$ for (41). Note that ε_m do not depend on the seesaw mass scale M_m except through α, Γ_1 and Γ_2. By adjusting the parameters a, b and α that are not constrained by observation, it is always possible to reproduce the baryon asymmetry $Y_B = 8.7 \times 10^{-11}$.

B. Nonthermal leptogenesis due to decaying right-handed scalar neutrinos

The mechanism described above operates when the right-handed neutrino masses M_1, M_2 are smaller than the reheating temperature which we assume in our scenario to be in the range $T_{\mathrm{RH}} = 10^5$–10^7 GeV. For larger M_1, M_2 the thermal leptogenesis scenario is not applicable as the right-handed (s)neutrinos do not thermalize. It is nevertheless possible to generate sufficient baryon asymmetry due to the decay of the right-handed sneutrinos that have acquired expectation values during inflation. In this sense our model is somewhat similar to the inflation model

[5]While this might seem enormous fine tuning, it can happen naturally as a result of renormalization group effects [66]. See also Ref. [67].

driven by the right-handed scalar neutrinos [36–38]. Indeed, for large seesaw scales the right-handed scalar neutrinos have noticeable contribution to the dynamics after the slow-roll, as shown in Fig. 1 for $M_1 = M_2 = 10^{13}$ GeV. Note, however, that the right-handed scalar neutrinos do not have to be involved in the inflationary dynamics.

In the supersymmetric SM including the right-handed neutrinos leptogenesis is automatic as long as the Hubble scale during inflation $H_{\rm inf}$ is larger than the right-handed neutrino mass scale [61], which is always the case in our model. Take, for example, the case of $M_1 = M_2 = 10^{13}$ GeV and $N_e = 60$ discussed in Sec. III B, which gives $r = 0.00296$. Using the CMB power spectrum $\Delta_R^2(k_0) = 2.43 \times 10^{-9}$, the Hubble parameter during inflation can be expressed in terms of the tensor-to-scalar ratio $r = 16\epsilon$ as $H_{\rm inf} = 2.67 \times \sqrt{r} \times 10^{14}$ GeV. With $r = 0.00296$ the Hubble parameter during inflation is larger than the right-handed neutrino masses, $H_{\rm inf} \approx 1.45 \times 10^{13}$ GeV $> M_1$, M_2. The seesaw relation (5) with the Yukawa coupling $\lesssim \mathcal{O}(1)$ constrains $M_1, M_2 \lesssim 10^{13}$ GeV, and for smaller M_1, M_2 the model yields larger r and hence larger $H_{\rm inf}$, so the inequality $H_{\rm inf} > M_1, M_2$ is satisfied more safely.

In this nonthermal leptogenesis scenario the right-handed scalar neutrinos acquire expectation values $\langle\tilde{N}\rangle$, either classically by the nontrivial inflaton trajectory, or due to the quantum fluctuation during inflation. This $\langle\tilde{N}\rangle$ can be regarded as the initial value of the right-handed scalar neutrinos that oscillate and decay. We shall assume $\langle\tilde{N}\rangle \lesssim M_{\rm Pl}$, where $M_{\rm Pl}$ is the Planck mass. Along with the decay of the right-handed scalar neutrinos the lepton asymmetry is generated, which is later converted into the baryon asymmetry by the $B - L$ conserving sphaleron process. The process of the decay actually depends on the decay rate of the inflaton Γ_φ and that of the right-handed neutrinos Γ_n. When (i) the scalar neutrino decay rate is larger than the inflaton decay rate $\Gamma_n > \Gamma_\varphi$, the scalar neutrinos decay during the reheating. When (ii) $\Gamma_n < \Gamma_\varphi < \Gamma_n(M_{\rm Pl}/\langle\tilde{N}\rangle)^4$, the scalar neutrinos decay after the reheating but do not dominate the energy density of the universe. When (iii) the scalar neutrino decay rate is much smaller $\Gamma_\varphi > \Gamma_n(M_{\rm Pl}/\langle\tilde{N}\rangle)^4$, the right-handed scalar neutrinos dominate the universe before they decay. In our model, the scalar neutrino decay rate[6] is (36) and the inflaton decay rate is estimated as $\Gamma_\varphi \approx 4$ MeV, assuming the Higgs $\longrightarrow b\bar{b}$ decay channel and the Higgs mass $\approx$ 125 GeV. It can be shown that in our scenario the case (iii) never occurs, as long as the inflaton trajectory is controlled to be nearly straight by the noncanonical Kähler terms. The threshold between (i) and (ii) is around $M_1 \approx M_2 \approx 10^{6.5}$ GeV, for typical values of the mass parameters $a = b = 1$ and for the normal or inverted mass hierarchy.

In both (i) and (ii) cases the yield of the lepton asymmetry is estimated as [61]

$$Y_L = \varepsilon_m \frac{\langle\tilde{N}\rangle^2}{M_m M_{\rm Pl}} \left(\frac{\Gamma_\varphi}{M_{\rm Pl}}\right)^{\frac{1}{2}}, \tag{42}$$

and the baryon asymmetry follows from (30). Assuming

$$\langle\tilde{N}\rangle^2 \simeq \frac{3H_{\rm inf}^4}{8\pi^2 M_m^2}, \tag{43}$$

generated by the quantum fluctuations,[7] the observed baryon asymmetry (1) with the condition for the CP asymmetry parameter $|\varepsilon_m| \lesssim 1$ leads to a mild upper bound on the seesaw mass scale $M_m \lesssim 10^{12}$ GeV.

V. THE INFLATON SELF COUPLING AND THE NEUTRINO MASS PARAMETERS

Our model of inflation is well approximated by the nonminimally coupled single field $\lambda\phi^4$ model. We have seen in Sec. III that the inflaton self coupling $\lambda = (y_D^\dagger y_D)_{kk}$ is related to the CMB spectrum, and argued that in the near future the value of λ will be constrained more severely by the observation. As λ is constructed from components of the Dirac Yukawa coupling, it is determined by the neutrino mass parameters. In this section we describe the relation between λ and these parameters.

We shall assume nearly degenerate right-handed neutrino mass parameters $M_1 \approx M_2$, which is favored for successful thermal leptogenesis as we discussed in the previous section. The matrix $M = \mathrm{diag}(M_1, M_2)$ is then proportional to the identity matrix and the relation (23) becomes

$$y_D^\dagger y_D \approx \frac{2M_1}{v^2 \sin^2\beta} U_{\rm MNS} \sqrt{D_\nu}^T R^\dagger R \sqrt{D_\nu} U_{\rm MNS}^\dagger. \tag{44}$$

Thus $(y_D^\dagger y_D)_{kk}$ is proportional to the seesaw mass parameter M_1. Essentially, the inflaton self coupling is determined by the seesaw mass scale [34]. Further complexity arises from the dependence on the other parameters b, δ and σ, which are not constrained by the present observation.

Dependence on a and b.—We first notice that λ does not depend on the parameter a. This is easily seen, as the product $R^\dagger R$ appearing in (44) is written as

$$R^\dagger R = \begin{pmatrix} \cosh 2b & i \sinh 2b \\ -i \sinh 2b & \cosh 2b \end{pmatrix}. \tag{45}$$

The coupling λ monotonically increases with $b > 0$. We show the behavior of $(y_D^\dagger y_D)_{kk}/M_1$ as functions of b

[6] Parametric resonance may enhance the decay rate. We do not consider such effects here.

[7] If $\langle\tilde{N}\rangle$ is set by the nontrivial inflaton trajectory as in the case of Fig. 1, the value of $\langle\tilde{N}\rangle$ depends on ζ. Then the lepton number generated through coherent oscillation and decay of the scalar neutrinos also depends on the parameter ζ.

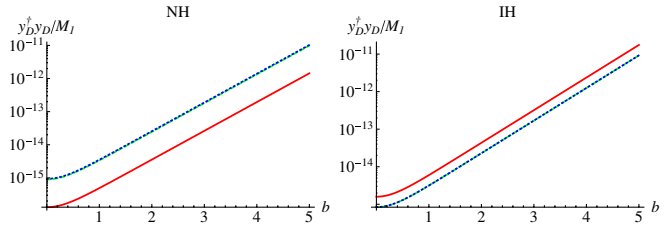

FIG. 6 (color online). Plot of $\lambda/M_1 \equiv (y_D^\dagger y_D)_{kk}/M_1$ (in GeV^{-1}) as functions of b. The Dirac and Majorana phases are chosen to be zero. The left panel is for the normal mass hierarchy and the right is for the inverted mass hierarchy. On each panel, the red solid, the green dashed, and the blue dotted curves indicate $k = 1, 2, 3$, respectively. The $k = 2$ and $k = 3$ curves overlie each other.

in Fig. 6, for $k = 1, 2, 3$, with the CP violating phases set to be $\delta = 0$, $\sigma = 0$. The self coupling λ changes by an order as b is shifted by 1; the dependence on b is thus significant.

Dependence on the Dirac phase δ.—The dependence of the inflaton self coupling λ on the Dirac phase δ is shown in Fig. 7, where $(y_D^\dagger y_D)_{kk}/M_1$ is plotted for $-\pi \le \delta < \pi$. We have chosen $b = 1$ and $\sigma = 0$. In the case of the normal mass hierarchy the $k = 1$ component is more susceptible than $k = 2, 3$, whereas for the inverted mass hierarchy $k = 2, 3$ are more susceptible than $k = 1$.

Dependence on the Majorana phase σ.—The inflaton self coupling λ also depends on the Majorana phase σ. In Fig. 8 we show the behavior of $(y_D^\dagger y_D)_{kk}/M_1$ as σ is varied from $-\pi$ to π. We have chosen $b = 1$ and $\delta = 0$.

To summarize, the inflaton self coupling λ depends on b, δ and σ but not on a. These parameters are not constrained by present experiments and thus introduce ambiguity in prediction of the model. Consider for instance the 2-σ contour in Fig. 3. For $N_e = 60$ this gives a constraint $\lambda = (y_D^\dagger y_D)_{kk} \gtrsim 10^{-12}$ which corresponds to $M_1 \approx M_2 \gtrsim 2$ TeV for $b = 1$, $\delta = \sigma = 0$, $k = 1$ in the normal mass hierarchy (Fig. 7). If we take $\delta = 1.6$ instead of $\delta = 0$, the 2-σ of CMB gives $M_1 \approx M_2 \gtrsim 20$ TeV.

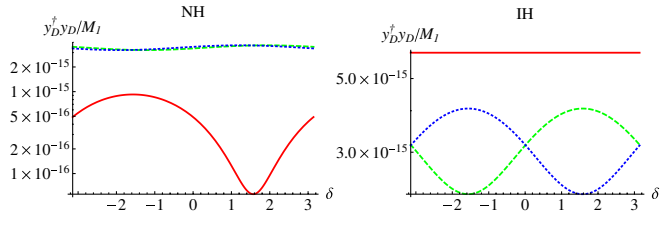

FIG. 7 (color online). Plot of $\lambda/M_1 \equiv (y_D^\dagger y_D)_{kk}/M_1$ for $k = 1$ (the red solid curves), $k = 2$ (green dashed) and $k = 3$ (blue dotted), as functions of the Dirac phase δ. The unit of λ/M_1 is in GeV^{-1}. The left panel shows the case for the normal mass hierarchy and the right panel is for the inverted mass hierarchy. We have chosen $b = 1$ and $\sigma = 0$.

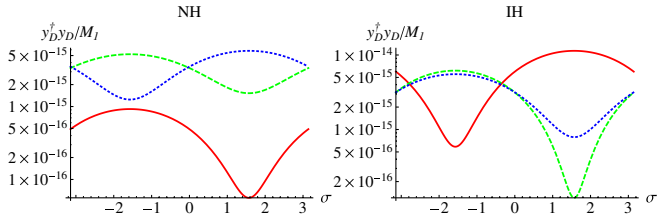

FIG. 8 (color online). Plot of $\lambda/M_1 \equiv (y_D^\dagger y_D)_{kk}/M_1$ for $k = 1$ (the red solid curves), $k = 2$ (green dashed), $k = 3$ (blue dotted), as functions of the Majorana phase σ. The unit of λ/M_1 is in GeV^{-1}. The left panel shows the case for the normal mass hierarchy and the right panel is for the inverted mass hierarchy. We have chosen $b = 1$ and $\delta = 0$.

VI. THE EFFECTS OF R-PARITY VIOLATION

While the seesaw model superpotential (2) preserves the R-parity (assuming the odd parity for the right-handed neutrino superfield), the Kähler potential (16) breaks it by the $\gamma_i L_i H_u$ terms. Small R-parity violation is known to be harmless, and it can often be beneficial [68–70]. It can nevertheless lead to difficulties and the consequences of introducing such terms need to be checked carefully. In this section we discuss viability of the scenario focusing on the effects of R-parity violation. We assume the canonical form of the Kähler terms for all the other chiral multiplets.

An immediate consequence of the $\gamma_i L_i H_u$ terms in the Kähler potential is that the Lagrangian includes the following terms:

$$\mathcal{L} \supset \int d^4\theta \phi^\dagger \phi (L_i^\dagger L_i + H_u^\dagger H_u + \gamma_i L_i H_u + \mathrm{H.c.})$$
$$= \int d^4\theta \left(L_i^\dagger L_i + H_u^\dagger H_u + \frac{\phi^\dagger}{\phi} \gamma_i L_i H_u + \mathrm{H.c.} \right), \quad (46)$$

where ϕ is the compensator in the superconformal formalism. To go from the first to the second line we have rescaled L_i, $H_u \to \phi^{-1} L_i$, $\phi^{-1} H_u$. When the supersymmetry is broken the compensator acquires an expectation value $\langle \phi \rangle = 1 + \theta^2 F_\phi$, where F_ϕ is the compensator F-term. The third term in (46) then becomes $\int d^4\theta (1 + \bar{\theta}^2 F_\phi^\dagger) \times (1 - \theta^2 F_\phi) \gamma_i L_i H_u$. This suggests generation of a bilinear R-parity breaking term $W_{\not R} = F_\phi^\dagger \gamma_i L_i H_u \equiv \mu_i L_i H_u$, as well as an R-parity breaking B-term $-|F_\phi|^2 \gamma_i \tilde{\ell}_i h_u$. In generic scenarios of supersymmetry breaking[8] the compensator F-term gives rise to the gravitino mass, $F_\phi \approx m_{3/2}$. Recalling that $\gamma_i = \gamma$ is related to the nonminimal coupling ξ by $\xi = \frac{\gamma}{4} - \frac{1}{6}$, we see $\gamma \approx 4\xi \gg 1$ when $\xi \gg 1$ and $\gamma \sim \mathcal{O}(1)$ when $\xi \lesssim 1$. We will assume $\gamma \sim \mathcal{O}(1)$ below, as one of the merits of our model was that the extremely large nonminimal coupling that could lead to the unitarity violation can be avoided. The bilinear

[8]There are exceptional cases, e.g., the almost no-scale model [71].

R-parity breaking term can then be written as $W_{\not R} \sim m_{3/2}\gamma_i L_i H_u \sim m_{3/2} L_k H_u$.

In the presence of the bilinear R-parity violating terms $W \sim H_u(\mu H_d + m_{3/2} L_k)$ the lepton number violating superpotential

$$W_{\Delta L=1} \sim (y_e^{ij}\varepsilon^k) e_i^c L_j L_k + (y_d^{ij}\varepsilon^k) d_i^c Q_j L_k, \qquad (47)$$

where $\varepsilon^k \sim m_{3/2}/\mu$, is generated. The cosmological constraints for these effective Yukawa couplings are [72–74]

$$y_e^{ij}\varepsilon^k, \qquad y_d^{ij}\varepsilon^k \lesssim 10^{-7}, \qquad (48)$$

from which one obtains $\varepsilon^k \sim m_{3/2}/\mu \lesssim 10^{-5}\cos\beta \sim 10^{-6}$. For a typical value of the MSSM μ parameter $\mu \sim 1$ TeV the gravitino mass of our model is

$$m_{3/2} \lesssim 1 \text{ MeV}. \qquad (49)$$

Thus, supersymmetry breaking mechanisms consistent with our scenario are those giving a small gravitino mass (such as the gauge mediation scenario). Note that the gravitinos with the small mass (49) are still a good candidate for the cold dark matter, even though the R-parity is broken.

The abundance of the thermally produced gravitinos is calculated as [75–77]

$$\Omega_{\tilde{G}} h^2 \simeq 0.3 \times \left(\frac{T_{\rm RH}}{10^{10}\text{ GeV}}\right)\left(\frac{100\text{ GeV}}{m_{3/2}}\right)\left(\frac{M_{\tilde{g}}}{1\text{ TeV}}\right)^2, \qquad (50)$$

where h is the Hubble parameter in the unit of 100 km Mpc^{-1} s^{-1} and $M_{\tilde{g}}$ is the running gluino mass. With $m_{3/2} \approx 1$ MeV and $M_{\tilde{g}} \approx 1$ TeV, the condition for avoiding the overdominance $\Omega_{\tilde{G}} h^2 \lesssim 0.1$ yields the upper bound of the reheating temperature $T_{\rm RH} \lesssim 10^5$ GeV. In a previous section we estimated the reheating temperature be $T_{\rm RH} \approx 10^5$–10^7 GeV, assuming the decay channel Higgs $\longrightarrow b\bar{b}$. The constraint of the gravitino abundance (50) suggests that $T_{\rm RH} \approx 10^5$ GeV is favored. Taking into account the Hubble expansion for the time needed for thermalization, $T_{\rm RH} \sim 10^5$ GeV seems to be a reasonable reheating temperature of our scenario. To summarize, our model typically predicts a scenario of gravitino cold dark matter with the reheating temperature $T_{\rm RH} \sim 10^5$ GeV. The smallness of the R-parity violating terms (48) guarantees that the baryon asymmetry generated by thermal/nonthermal leptogenesis remains without being wiped out.

We close this section with two comments. First, the constraint on the R-parity violation (48) does not have to be taken too strict since, for example, details of the flavor structure may slightly relax this condition [78]. Our second comment concerns the effects on the neutrino masses. R-parity violation induces neutrino masses without invoking right-handed neutrinos [79–84]. This alternative mechanism to the seesaw can be a potential threat, since if such an effect dominates over the usual seesaw mechanism that would give unacceptably large neutrino masses. A back-of-the-envelope calculation shows that there is actually no such danger, as the constraint (48) is more stringent than the one coming from the neutrino masses. For example, in the bilinear R-parity breaking scenario [85–87] the condition on the bilinear coefficient μ_i for not generating too large neutrino masses is $\mu_i/\mu \lesssim 10^{-3} \gg 10^{-6}$.

VII. DISCUSSION

We have discussed in this paper a simple model of inflationary cosmology based on the supergravity-embedded minimal seesaw model. The scenario is economical as it simultaneously explains various issues—neutrino oscillation, the origin of the baryon asymmetry and the origin of the cold dark matter—apart from the standard issues of big bang cosmology solved by inflation. We have shown that the model reproduces observationally acceptable values of the cosmological parameters, and argued that the prediction for n_s, r of the CMB spectrum will be tested by satellite experiments in the near future. A particularly interesting feature of this model is that the seesaw mass scale is constrained by the CMB. Thus far useful constraints on the (left-handed) neutrinos, such as the total neutrino masses $\sum m_\nu$ and the effective number of the neutrino species, have been obtained by observing the CMB and the large scale structure. However, the nature of the right-handed neutrons remains mysterious: being gauge singlets, their detection in colliders is virtually impossible, nevertheless they are essential for both seesaw mechanism and leptogenesis. In our proposal, the CMB may provide access to the physics of the right-handed neutrinos.

A key feature of our model is the nonminimal coupling of the D-flat direction inflaton to the background gravitational curvature, which is naturally implemented by supergravity embedding of the SM. In contrast to the nonminimally coupled Higgs inflation type models, the coupling in our case need not be large. This is related to the fact that the Dirac Yukawa coupling can be very small. Such extremely small Yukawa coupling is, nevertheless, not unnatural. The Dirac Yukawa coupling corresponding to a TeV scale right-handed neutrino mass in our model is in the same order as the electron Yukawa coupling. As Nature allows such a small coupling for the electrons, there is no reason to exclude the Dirac Yukawa coupling of the same order for the neutrinos.

Finally, we comment on extension of our model in various directions. While embedding into the $SO(10)$ grand unified theory is not possible, one may for example consider our scenario in the grand unified theory of $SU(5)$ plus a singlet. Also, type III seesaw with $SU(5)$ adjoint neutrinos in $SU(5)$ is possible. It is also straightforward to extend our model to the right-handed neutrinos with three families. An obvious drawback of such an extension is that the inflationary scenario will contain more unconstrained

parameters and the predictive power of the model will be reduced.

ACKNOWLEDGMENTS

S. K. acknowledges helpful conversations with Alejandro Ibarra, Shinta Kasuya, Kazunori Kohri and Masahide Yamaguchi. This research was supported in part by the Research Program MSM6840770029 the project of International Cooperation ATLAS-CERN of the Ministry of Education, Youth and Sports of Czech Republic, the JSPS - ASCR Japan - Czech Republic Research Cooperative Program (M. A.), the National Research Foundation of Korea Grant-in-Aid for Scientific Research No. 2012-007575 (S. K.) and by the DOE Grant No. DE-FG02-10ER41714 (N. O.). A part of the numerical computation was carried out using computing facilities at the Yukawa Institute, Kyoto University.

APPENDIX: BOLTZMANN EQUATIONS

We discussed leptogenesis within our inflationary scenario in Sec. IVA and presented the solutions of the Boltzmann equations. In this appendix we collect related formulas. The Boltzmann equations in the context of leptogenesis are discussed in Refs. [88–90]. We follow the conventions of Plumacher [63].

In the supersymmetric minimal seesaw model the dominant processes for generating the lepton number are the decay of the right-handed Majorana neutrino N_m into the up-type Higgs boson and a lepton, or into the higgsino and a scalar lepton:

$$N_m \to H_u + \ell, \qquad \tilde{\bar{h}} + \tilde{\ell}, \tag{A1}$$

as well as the decay of its superpartner $\widetilde{N}^c_j$ into the higgsino and a lepton, or into the Higgs boson and a scalar lepton:

$$\widetilde{N}^c_m \to H_u + \tilde{\ell}, \qquad \tilde{h} + \bar{\ell}. \tag{A2}$$

The decay widths for these processes are

$$\Gamma_m = \frac{M_m}{4\pi}(y_D y_D^\dagger)_{mm}. \tag{A3}$$

It is convenient to parametrize the inverse temperature using the right-handed neutrino mass M_1 as

$$z \equiv \frac{M_1}{T}. \tag{A4}$$

In the out-of-equilibrium decay of the right-handed neutrinos and sneutrinos, we assume the initial number densities of the leptons Y_{L_f} and sleptons Y_{L_s} to be zero. We also assume that the right-handed sneutrinos are initially symmetric: $Y_{\widetilde{N}^c_m} = Y_{\widetilde{N}^c_m}{}^\dagger$. Ignoring subdominant processes, it follows that $Y_{\widetilde{N}^c_m} = Y_{\widetilde{N}^c_m}{}^\dagger$ persists during the subsequent evolution. The Boltzmann equations for the number densities of the right-handed (s)neutrinos and the (s)lepton numbers then read

$$\frac{dY_{N_m}}{dz} = -\frac{z}{sH(M_1)}\left(\frac{Y_{N_m}}{Y^{\rm eq}_{N_m}} - 1\right)\gamma_{N_m}, \tag{A5}$$

$$\frac{dY_{\tilde{N}^c_m}}{dz} = -\frac{z}{sH(M_1)}\left(\frac{Y_{\tilde{N}^c_m}}{Y^{\rm eq}_{\tilde{N}^c_m}} - 1\right)\gamma_{N_m}, \tag{A6}$$

$$\frac{dY_{L_f}}{dz} = -\frac{z}{sH(M_1)}\sum_m\left\{\left(\frac{1}{2}\frac{Y_{L_f}}{Y^{\rm eq}_{\ell}} + \varepsilon_m\right)\gamma_{N_m} - \frac{1}{2}\left(\frac{Y_{N_m}}{Y^{\rm eq}_{N_m}} + \frac{Y_{\tilde{N}^c_m}}{Y^{\rm eq}_{\tilde{N}^c_m}}\right)\varepsilon_m\gamma_{N_m}\right\}, \tag{A7}$$

$$\frac{dY_{L_s}}{dz} = -\frac{z}{sH(M_1)}\sum_m\left\{\left(\frac{1}{2}\frac{Y_{L_s}}{Y^{\rm eq}_{\tilde{\ell}}} + \varepsilon_m\right)\gamma_{N_m} - \frac{1}{2}\left(\frac{Y_{N_m}}{Y^{\rm eq}_{N_m}} + \frac{Y_{\tilde{N}^c_m}}{Y^{\rm eq}_{\tilde{N}^c_m}}\right)\varepsilon_m\gamma_{N_m}\right\}. \tag{A8}$$

Here, $H(M_1)$ is the Hubble parameter at temperature $T = M_1$ and

$$\gamma_{N_m} = n^{\rm eq}_{N_m}\frac{K_1(z)}{K_2(z)}\Gamma_m, \tag{A9}$$

is the reaction density of the decay processes. K_1, K_2 are the elliptic integrals of the first and the second kind. The Boltzmann equations (A5) and (A6), as well as (A7) and (A8), are identical to each other due to supersymmetry.

We solved the above equations with the yields in equilibrium,

$$Y^{\rm eq}_{N_m} = Y^{\rm eq}_{\tilde{N}^c_m} = \frac{n^{\rm eq}_{N_m}}{s}, \qquad n^{\rm eq}_{N_m} = \frac{M_1^3}{\pi^2 z}K_2(z), \tag{A10}$$

$$Y^{\rm eq}_{\ell} = Y^{\rm eq}_{\tilde{\ell}} = \frac{n^{\rm eq}_{\ell}}{s}, \qquad n^{\rm eq}_{\ell} = \frac{2}{\pi^2}\left(\frac{M_1}{z}\right)^3. \tag{A11}$$

These Boltzmann equations assume supersymmetry and are not strictly applicable below the supersymmetry breaking scale $T \sim$ TeV. The deviation from the supersymmetric case is however expected to be minor as it should naturally be within a factor of 2.

[1] L. McAllister and E. Silverstein, Gen. Relativ. Gravit. **40**, 565 (2008).
[2] A. Ashtekar and P. Singh, Classical Quantum Gravity **28**, 213001 (2011).
[3] J. J. Heckman, A. Tavanfar, and C. Vafa, J. High Energy Phys. 04 (2010) 054.
[4] C. Bennett, D. Larson, J. Weiland, N. Jarosik, G. Hinshaw *et al.*, arXiv:1212.5225.
[5] G. Hinshaw, D. Larson, E. Komatsu, D. Spergel, C. Bennett *et al.*, arXiv:1212.5226.
[6] J. L. Cervantes-Cota and H. Dehnen, Nucl. Phys. **B442**, 391 (1995).
[7] F. L. Bezrukov and M. Shaposhnikov, Phys. Lett. B **659**, 703 (2008).
[8] A. Barvinsky, A. Kamenshchik, and A. Starobinsky, J. Cosmol. Astropart. Phys. 11 (2008) 021.
[9] A. De Simone, M. P. Hertzberg, and F. Wilczek, Phys. Lett. B **678**, 1 (2009).
[10] F. Bezrukov and M. Shaposhnikov, J. High Energy Phys. 07 (2009) 089.
[11] F. Bezrukov, A. Magnin, M. Shaposhnikov, and S. Sibiryakov, J. High Energy Phys. 01 (2011) 016.
[12] A. O. Barvinsky, A. Y. Kamenshchik, C. Kiefer, A. A. Starobinsky, and C. Steinwachs, J. Cosmol. Astropart. Phys. 12 (2009) 003.
[13] A. Barvinsky, A. Kamenshchik, C. Kiefer, A. Starobinsky, and C. Steinwachs, Eur. Phys. J. C **72**, 2219 (2012).
[14] J. L. F. Barbon and J. R. Espinosa, Phys. Rev. D **79**, 081302 (2009).
[15] C. P. Burgess, H. M. Lee, and M. Trott, J. High Energy Phys. 09 (2009) 103.
[16] C. P. Burgess, H. M. Lee, and M. Trott, J. High Energy Phys. 07 (2010) 007.
[17] M. P. Hertzberg, J. High Energy Phys. 11 (2010) 023.
[18] R. N. Lerner and J. McDonald, J. Cosmol. Astropart. Phys. 04 (2010) 015.
[19] R. N. Lerner and J. McDonald, Phys. Rev. D **82**, 103525 (2010).
[20] A. A. Starobinsky, Phys. Lett. **91B**, 99 (1980).
[21] B. Spokoiny, Phys. Lett. **147B**, 39 (1984).
[22] T. Futamase and K.-i. Maeda, Phys. Rev. D **39**, 399 (1989).
[23] D. S. Salopek, J. R. Bond, and J. M. Bardeen, Phys. Rev. D **40**, 1753 (1989).
[24] N. Makino and M. Sasaki, Prog. Theor. Phys. **86**, 103 (1991).
[25] G. Aad *et al.* (ATLAS Collaboration), Phys. Lett. B **716**, 1 (2012).
[26] S. Chatrchyan *et al.* (CMS Collaboration), Phys. Lett. B **716**, 30 (2012).
[27] S. Ferrara, R. Kallosh, A. Linde, A. Marrani, and A. Van Proeyen, Phys. Rev. D **82**, 045003 (2010).
[28] S. Ferrara, R. Kallosh, A. Linde, A. Marrani, and A. Van Proeyen, Phys. Rev. D **83**, 025008 (2011).
[29] M. B. Einhorn and D. R. T. Jones, J. High Energy Phys. 03 (2010) 026.
[30] M. Arai, S. Kawai, and N. Okada, Phys. Rev. D **84**, 123515 (2011).
[31] M. B. Einhorn and D. T. Jones, J. Cosmol. Astropart. Phys. 11 (2012) 049.
[32] C. Pallis and N. Toumbas, J. Cosmol. Astropart. Phys. 02 (2011) 019.
[33] P. Minkowski, Phys. Lett. **67B**, 421 (1977); T. Yanagida, in *Proceedings of the Workshop on the Baryon Number of the Universe and Unified Theories, Tsukuba, Japan, 1979*, edited by O. Sawada and A. Sugamoto, KEK Report No. KEK-79-18, p. 95; M. Gell-Mann, P. Ramond, and R. Slansky, in *Supergravity*, edited by P. van Nieuwenhuizen and D. Z. Freedman (North Holland, Amsterdam, 1979), pp. 315–321; R. N. Mohapatra and G. Senjanovic, Phys. Rev. Lett. **44**, 912 (1980).
[34] M. Arai, S. Kawai, and N. Okada, Phys. Rev. D **86**, 063507 (2012).
[35] P. Frampton, S. Glashow, and T. Yanagida, Phys. Lett. B **548**, 119 (2002).
[36] H. Murayama, H. Suzuki, T. Yanagida, and J. Yokoyama, Phys. Rev. Lett. **70**, 1912 (1993).
[37] H. Murayama, H. Suzuki, T. Yanagida, and J. Yokoyama, Phys. Rev. D **50**, R2356 (1994).
[38] J. R. Ellis, M. Raidal, and T. Yanagida, Phys. Lett. B **581**, 9 (2004).
[39] R. Allahverdi, K. Enqvist, J. Garcia-Bellido, and A. Mazumdar, Phys. Rev. Lett. **97**, 191304 (2006).
[40] R. Allahverdi, K. Enqvist, J. Garcia-Bellido, A. Jokinen, and A. Mazumdar, J. Cosmol. Astropart. Phys. 06 (2007) 019.
[41] R. Allahverdi, A. Kusenko, and A. Mazumdar, J. Cosmol. Astropart. Phys. 07 (2007) 018.
[42] J. Bueno Sanchez, K. Dimopoulos, and D. H. Lyth, J. Cosmol. Astropart. Phys. 01 (2007) 015.
[43] M. Fukugita and T. Yanagida, Phys. Lett. B **174**, 45 (1986).
[44] M. Flanz, E. A. Paschos, U. Sarkar, and J. Weiss, Phys. Lett. B **389**, 693 (1996).
[45] A. Pilaftsis, Phys. Rev. D **56**, 5431 (1997).
[46] A. Pilaftsis and T. E. J. Underwood, Nucl. Phys. **B692**, 303 (2004).
[47] K. Nakamura *et al.* (Particle Data Group), J. Phys. G **37**, 075021 (2010).
[48] F. An *et al.* (DAYA-BAY Collaboration), Phys. Rev. Lett. **108**, 171803 (2012).
[49] J. Casas and A. Ibarra, Nucl. Phys. **B618**, 171 (2001).
[50] A. Ibarra and G. G. Ross, Phys. Lett. B **591**, 285 (2004).
[51] M. Kaku, P. K. Townsend, and P. van Nieuwenhuizen, Phys. Rev. D **17**, 3179 (1978); W. Siegel and S. J. Gates, Jr., Nucl. Phys. **B147**, 77 (1979); E. Cremmer, S. Ferrara, L. Girardello, and A. Van Proeyen, Nucl. Phys. **B212**, 413 (1983); S. Ferrara, L. Girardello, T. Kugo, and A. Van Proeyen, Nucl. Phys. **B223**, 191 (1983); T. Kugo and S. Uehara, Nucl. Phys. **B222**, 125 (1983); **B226**, 49 (1983); Prog. Theor. Phys. **73**, 235 (1985).
[52] N. Okada, M. U. Rehman, and Q. Shafi, Phys. Rev. D **82**, 043502 (2010).
[53] S. Hotchkiss, A. Mazumdar, and S. Nadathur, J. Cosmol. Astropart. Phys. 06 (2011) 002; A. Mazumdar and S. Morisi, Phys. Rev. D **86**, 045031 (2012).
[54] Planck Collaboration, arXiv:astro-ph/0604069, URL http://www.rssd.esa.int/index.php?project=Planck.
[55] P. A. R. Ade *et al.* (Planck Collaboration), Astron. Astrophys. **536**, A1 (2011).

[56] Z. Kermish, P. Ade, A. Anthony, K. Arnold, K. Arnold *et al.*, arXiv:1210.7768.
[57] M. Hazumi, AIP Conf. Proc. **1040**, 78 (2008).
[58] B. A. Bassett and S. Liberati, Phys. Rev. D **58**, 021302 (1998).
[59] S. Tsujikawa, K.-i. Maeda, and T. Torii, Phys. Rev. D **60**, 063515 (1999).
[60] R. Allahverdi, A. Ferrantelli, J. Garcia-Bellido, and A. Mazumdar, Phys. Rev. D **83**, 123507 (2011).
[61] H. Murayama and T. Yanagida, Phys. Lett. B **322**, 349 (1994).
[62] I. Affleck and M. Dine, Nucl. Phys. **B249**, 361 (1985).
[63] M. Plumacher, Nucl. Phys. **B530**, 207 (1998).
[64] W. Buchmuller, P. Di Bari, and M. Plumacher, Nucl. Phys. **B643**, 367 (2002).
[65] W. Buchmuller, P. Di Bari, and M. Plumacher, Ann. Phys. (Amsterdam) **315**, 305 (2005).
[66] R. Gonzalez Felipe, F. Joaquim, and B. Nobre, Phys. Rev. D **70**, 085009 (2004).
[67] N. Okada, Y. Orikasa, and T. Yamada, Phys. Rev. D **86**, 076003 (2012).
[68] H. K. Dreiner, arXiv:hep-ph/9707435.
[69] R. Barbier, C. Berat, M. Besancon, M. Chemtob, A. Deandrea *et al.*, Phys. Rep. **420**, 1 (2005).
[70] W. Buchmuller, L. Covi, K. Hamaguchi, A. Ibarra, and T. Yanagida, J. High Energy Phys. 03 (2007) 037.
[71] M. A. Luty and N. Okada, J. High Energy Phys. 04 (2003) 050.
[72] B. A. Campbell, S. Davidson, J. R. Ellis, and K. A. Olive, Phys. Lett. B **256**, 484 (1991).
[73] W. Fischler, G. Giudice, R. Leigh, and S. Paban, Phys. Lett. B **258**, 45 (1991).
[74] H. K. Dreiner and G. G. Ross, Nucl. Phys. **B410**, 188 (1993).
[75] M. Bolz, A. Brandenburg, and W. Buchmuller, Nucl. Phys. **B606**, 518 (2001).
[76] J. Pradler and F. D. Steffen, Phys. Rev. D **75**, 023509 (2007).
[77] F. D. Steffen, J. Cosmol. Astropart. Phys. 09 (2006) 001.
[78] M. Endo, K. Hamaguchi, and S. Iwamoto, J. Cosmol. Astropart. Phys. 02 (2010) 032.
[79] L. J. Hall and M. Suzuki, Nucl. Phys. **B231**, 419 (1984).
[80] I.-H. Lee, Phys. Lett. **138B**, 121 (1984).
[81] I.-H. Lee, Nucl. Phys. **B246**, 120 (1984).
[82] S. Dawson, Nucl. Phys. **B261**, 297 (1985).
[83] C. Aulakh and R. N. Mohapatra, Phys. Lett. **119B**, 136 (1982).
[84] J. R. Ellis, G. Gelmini, C. Jarlskog, G. G. Ross, and J. Valle, Phys. Lett. **150B**, 142 (1985).
[85] R. Hempfling, Nucl. Phys. **B478**, 3 (1996).
[86] H.-P. Nilles and N. Polonsky, Nucl. Phys. **B484**, 33 (1997).
[87] M. Hirsch, M. Diaz, W. Porod, J. Romao, and J. Valle, Phys. Rev. D **62**, 113008 (2000).
[88] E. W. Kolb and S. Wolfram, Nucl. Phys. **B172**, 224 (1980).
[89] A. Dolgov and Y. Zeldovich, Rev. Mod. Phys. **53**, 1 (1981).
[90] M. Luty, Phys. Rev. D **45**, 455 (1992).